PCCP

PAPER

View Article Online
View Journal | View Issue

Cite this: *Phys. Chem. Chem. Phys.*, 2023, **25**, 12041

A new green-to-blue upconversion system with efficient photoredox catalytic properties†

Jorge Castellanos-Soriano, [a] Till J. B. Zähringer, [b] Jorge C. Herrera-Luna, [a] M. Consuelo Jiménez, [a] Christoph Kerzig *[b] and Raúl Pérez-Ruiz *[a]

Received 21st February 2023,
Accepted 4th April 2023

DOI: 10.1039/d3cp00811h

rsc.li/pccp

The design and development of new triplet–triplet annihilation upconversion (TTA-UC) systems combining triplet sensitizers with acceptor compounds have attracted considerable interest. In this vein, sensitizers made from purely organic dyes rather than transition-metal complexes appear to be more convenient from an environmental point of view. BODIPYs are a very well-known class of dyes with applications in a widespread range of scientific areas. Owing to the versatility of BODIPYs, we present herein a new asymmetric BODIPY with excellent photophysical properties to be used as an appropriate sensitizer in a bimolecular TTA-UC system. Detailed spectroscopic measurements demonstrated the ability of this new design to sensitize TTA-UC by combination with a suitable acceptor such as 2,5,8,11-tetra-*tert*-butylperylene (**TBPe**), allowing a successful conversion of green to blue light. The singlet-excited **TBPe** so obtained is capable of activating aryl chlorides reductively which initiated the functionalization of *N*-methylpyrrole (Meerwein-type arylation) and formation of both substituted triarylethylenes (Mizoroki–Heck reaction) and heteroarene phosphonates (photo-Arbuzov reaction). Product yields reveal that our TTA-UC system behaved as a highly efficient photocatalytic entity.

Introduction

Photon upconversion based on triplet–triplet annihilation (TTA-UC) has attracted considerable interest in the last decade due to its applicability to a broad range of scientific areas such as anticounterfeiting,[1] solar fuels,[2,3] photovoltaics,[4–7] biophotonics,[8–12] and more recently in photoredox catalysis.[13–15] The motivation for employing this phenomenon is mainly due to two reasons: (i) the development of numerous TTA-UC systems (from hybrid organic/inorganic to purely organic materials) that provide lots of chances for their applications,[16] and (ii) the high efficiency at low excitation intensities with non-coherent light[17,18] in comparison with other UC systems based on two-photon absorption.[19]

Typical TTA-UC implies the association of multistep photochemical events (Fig. 1A). After absorption of low energy photons ($h\nu_1$), the triplet excited state (T_1) of the sensitizer (or a donor) is produced by intersystem crossing (ISC) from the singlet excited state (S_1). Subsequently, triplets of the annihilator (or an acceptor) are populated through triplet–triplet energy transfer (TTEnT) from the triplets of the sensitizer (the Dexter mechanism). When two annihilator molecules at their triplet states are able to collide during their lifetimes, a higher singlet energy level is formed by means of triplet–triplet annihilation (TTA) and delayed upconverted fluorescence ($h\nu_2$) is consequently generated. The emission energy of the new photon is greater than the energy of the initially absorbed photon, making this procedure one of the most attractive wavelength conversion technologies.

Based on the literature data, Pd and Pt porphyrins as sensitizers[20] coupled with organic emitters like rubrene,[21] perylene[22] and diphenylanthracene[23] are found to be the most common TTA-UC systems. The triplet formation of the sensitizers occurs efficiently *via* spin–orbital interactions promoted by the heavy atoms (noble metals such as Pd and Pt), permitting the UC luminescence of the system. Investigations regarding other sensitizers such as semiconductor nanocrystals,[24] quantum dots,[25] perovskites,[26] lanthanide complexes,[27] complexes with more earth-abundant metals,[28,29] molecules showing TADF (thermally activated delayed fluorescence),[30] and electron donor–acceptor dyads[31] have also been reported. Most of these systems require expensive and complex sensitizers, presenting somehow several drawbacks including low photostability, structural instability, and a limited usable range of solvent conditions. Therefore, the employment of more readily available and organic sensitizers with high extinction coefficients in the appropriate absorption region, high photostability, and

[a] *Departamento de Química, Universitat Politècnica de Valencia, Camino de Vera S/N, 46022, Valencia, Spain. E-mail: raupreru@upv.es*
[b] *Department of Chemistry, Johannes Gutenberg University Mainz, Duesbergweg 10-14, 55128, Mainz, Germany. E-mail: ckerzig@uni-mainz.de*

† Electronic supplementary information (ESI) available. CCDC 2236113 and 2236116. For ESI and crystallographic data in CIF or other electronic format see DOI: https://doi.org/10.1039/d3cp00811h

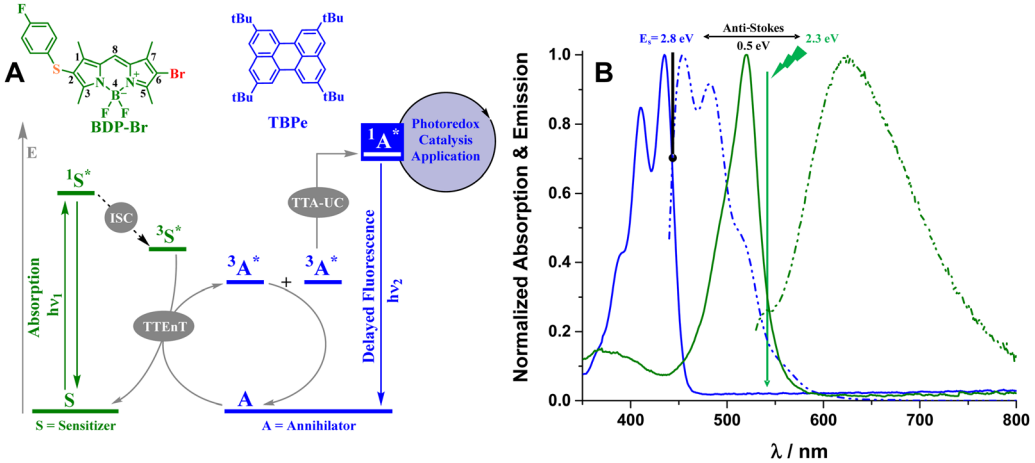

Fig. 1 (A): Schematic representation of the corresponding photophysical events associated with the TTA-UC phenomenon enabled by the **BDP-Br** (sensitizer) and **TBPe** (annihilator) pair and its implementation in photoredox catalysis. (B): Normalized absorption (solid line) and emission (dashed dotted line) spectra of **BDP-Br** (green) and **TBPe** (blue) in 8 μM aerated acetonitrile/dimethylacetamide (4/1 v/v) solution.

insensitivity to solvent environments appears to be more desirable.

In this context, boron dipyrromethene (BODIPY) derivatives fulfill the abovementioned criteria and the addition of halogen substituents (the so-called internal heavy-atom effect)[32] directly onto the chromophore, not to the peripheral moieties, provides a direct effect on the ISC quantum yield and the population of triplets substantially enhances.[33–35] Thus, the number of reports on the photosensitization of TTA-UC using BODIPY-based donors has increased over the last few years.[36,37] Encouraged by this continuous evolution and on the basis of the viable and straightforward functionalization of the BODIPY framework, it would be of great interest to construct new BODIPY dyes with special properties to be used as suitable sensitizers in a bimolecular TTA-UC system.

As a matter of fact, we have herein prepared an asymmetric BODIPY (6-bromo-2-(4-fluorophenyl)thio-1,3,5,7-tetramethyl-4,4-difluoro-4-bora-3*a*,4*a*-diaza-*s*-indacene, **BDP-Br**, Fig. 1A) in which the presence of heteroatoms such as sulfur atoms plus one bromine is expected to not only alter the energy level of the triplet state but also shift the UV-Vis absorption band to the green region. This molecular design permits a lower energetic light input ($\lambda_{exc} > 530$ nm) and milder reaction conditions, while avoiding iodine atoms that frequently result in rather photolabile dyes. The ability to successfully sensitize TTA-UC in solution has been demonstrated through spectroscopic methods, employing an adequate acceptor such as 2,5,8,11-tetra-*tert*-butylperylene (**TBPe**).

Moreover, the generation of highly energetic species by this phenomenon (Fig. 1B) seems useful for the application of photoredox catalysis *via* upconversion. Hence, the activation of an aryl chloride with a high-energy demanding bond using this novel TTA-UC couple has led to different chemical transformations such as *N*-methylpyrrole functionalization, the production of a triarylethylene compound and the formation of a new C–P bond. These three overall redox-neutral reactions have been investigated based on product analysis and spectroscopic measurements, supporting the relationship between the photophysical (ISC, TTEnT, and TTA) and photochemical (SET, radical trapping, and C–C or C–P couplings) events.

Results and discussion

Synthesis of BDP-Br

As stated above, one of the main goals in this study was to synthesize a new BODIPY-like sensitizer to be involved in a bimolecular system for TTA-UC purposes. Interestingly, this new entity possesses an asymmetric structure with a 4-fluorophenyl sulfide group attached to one side of the chromophore whereas a bromine atom was attached to the opposite side of the chromophore. This disposition conferred a particular electronic density with the occurrence of strong absorption of visible light, an efficient ISC, and a long-lived triplet state.

Based on the reported data on sulfenylation of pyrroles catalyzed by copper,[38] the addition of 4-fluorothiophenol to the starting material 3,5-dimethylpyrrole-2-carboxaldehyde was first carried out, obtaining a 50% yield of the corresponding product **A** (Fig. 2). The next step was crucial in the construction of an asymmetrical structure and the condensation of compound **A** with 2,4-dimethylpyrrole led to the formation of intermediate dipyrromethane **B** with 68% yield. Now, the treatment of **B** with a base such as triethylamine followed by boron trifluoride diethyl etherate[39] yielded 66% of the BODIPY derivative **BDP** (2-(4-fluorophenyl)thio-1,3,5,7-tetramethyl-4,4-difluoro-4-bora-3*a*,4*a*-diaza-*s*-indacene, Fig. 2) whose structure was confirmed by X-ray analysis. The last step consisted of the addition of a bromine atom to **BDP** by NBS (*N*-bromosuccinimide) treatment and the target compound **BDP-Br** was quantitatively obtained. The location of bromine at position 6 was successfully supported by X-ray analysis (Fig. 2). It should be noted that structural determination by single-crystal X-ray diffraction revealed not only that both BODIPY species crystallise in the triclinic space group $P\bar{1}$ but also the planarity of the

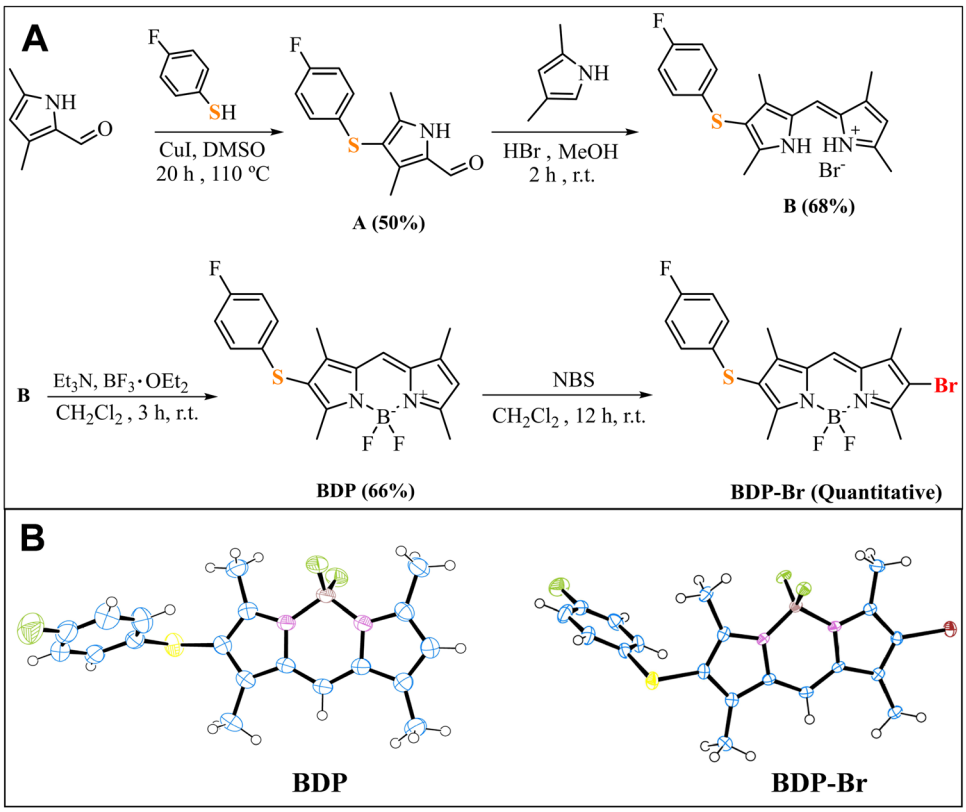

Fig. 2 (A): Synthetic route for the formation of **BDP-Br**. For more details on the synthetic procedures, see the ESI.† (B): ORTEP pictures of the X-ray structures of **BDP** and **BDP-Br**.

BODIPY core was confirmed which was extended through the bromine group in the case of **BDP-Br**. Thus, the design of **BDP-Br** could have a high impact on the ISC quantum yield. On the one hand, the presence of the 4-fluorophenyl sulfide group would give rise to a weakly emissive twisted intramolecular charge-transfer excited state (TICT)[40] between the sulfur's lone electron pair and an excited electron-deficient BODIPY moiety. On the other hand, chromophore structures bearing heavy atoms such as Br would affect directly the triplet state lifetime of the molecule and would stabilize the ISC process.[41] Therefore, **BDP-Br** appears to be the ideal choice to be applied to both TTA-UC and photoredox catalysis.

General photophysical and photochemical properties of BDP-Br

Regarding optical characterization, we investigated the photophysical properties of **BDP-Br**, which include absorption/emission bands, molar absorption coefficients, Stokes shifts, fluorescence quantum yields, emission rate constants, singlet energies and lifetimes in different solvents (Table 1). The absorption spectra of **BDP-Br** in all solvents presented an absorption band ($\lambda_{max.abs}$) in the green region (517–527 nm), being only weakly dependent on the solvent polarity (see Fig. S5 in the ESI†). It displayed molar extinction coefficients (ε), Stokes shifts ($\Delta\bar{\nu}$) and fluorescence lifetimes in the same order of magnitude as found for similar BODIPYs.[40] Interestingly, lower absolute fluorescence quantum yields (Φ_F) were obtained in more polar solvents, suggesting that the intersystem crossing efficiency from the lowest singlet excited state to the triplet would be enhanced by the internal heavy-atom effect or the formation of a TICT state. Besides, the phosphorescence spectrum of **BDP-Br** in the ethanol matrix at 77 K was recorded at λ_{max} of 780 nm (Fig. S6 in the ESI†), and was in accordance with those of halogen-substituted BODIPYs previously reported.[42] Furthermore, the lowest triplet energy (E_T) of **BDP-Br** was estimated to be 1.68 eV, which was found to be larger than that of **TBPe** (1.53 eV)[15] and makes energy transfer possible from the T_1 of **BDP-Br** to the T_1 of **TBPe**.

Table 1 Photophysical properties of **BDP-Br**

Solvent	$\lambda_{max.abs}$ [a]	$\lambda_{max.em}$ [a]	ε [b]	$\Delta\bar{\nu}$ [c]	E_S [d]	Φ_F [e]	τ_F [f]	k_F [g]
MeOH	517	612	44 600	3003	2.30	0.05	2.1	2.4×10^7
ACN	520	614	29 500	2944	2.18	0.05	2.0	2.0×10^7
DMSO	522	630	25 070	3284	2.25	0.04	2.5	1.6×10^7
DMA	525	625	66 670	3048	2.21	0.04	2.2	1.8×10^7
DCM	525	609	26 700	2628	2.27	0.10	2.3	4.3×10^7
Hexane	527	587	25 070	1939	2.28	0.30	3.5	8.5×10^7
ACN/DMA (4 : 1)	524	625	36 600	3084	2.26	0.04	2.5	1.6×10^7

[a] Maximum absorption/emission peak (in nm). [b] Molar extinction coefficient (in M^{-1} cm^{-1}). [c] Stokes shifts (in cm^{-1}). [d] Singlet energy (in eV). [e] Absolute fluorescence quantum yield. [f] Singlet lifetime (in ns). [g] Fluorescence rate constant (in s^{-1}). MeOH: methanol; DMSO: dimethylsulfoxide; DCM: dichloromethane; DMA: *N*,*N*-dimethylacetamide; ACN: acetonitrile.

To investigate the inherent photostability of the novel sensitizer, comparative stability measurements under monochromatic green light excitation with the widely used reference compound $[Ru(bpy)_3](PF_6)_2$ were carried out.[43] These semi-quantitative studies (Fig. S10, ESI†) revealed the outstanding photostability of **BDP-Br** – its photodegradation quantum yield is lower than that of the (already quite stable) $[Ru(bpy)_3]^{2+}$ by about two orders of magnitude.

ISC quantum yield of BDP-Br

One of the key parameters to determine the TTA-UC efficiency is the ISC quantum yield (Φ_{ISC}) of the sensitizer. This value is regularly estimated by singlet oxygen measurements in an indirect fashion, whereas a direct method can yield more reliable results. In this context, the Φ_{ISC} of **BDP-Br** was determined using laser flash photolysis actinometry[44,45] with the well-defined Φ_{ISC} of $[Os(phen)_3](PF_6)_2$ as the reference system. Briefly, this method is based on identical excitation conditions at a laser wavelength of 532 nm (Fig. 3A), adding a known concentration of **TBPe** (10 mM) to the sensitizers. Then, the triplet energy transfer efficiency η_{TTEnT} is compared after excitation (Fig. 3B and C) and the generation of the triplet-excited perylene[46] is detected using transient absorption spectroscopy (*vide infra* for more detailed TTEnT measurements with the **BDP-Br–TBPe** pair). Since we are using the same acceptor, the relative concentration of the generated ^{3}**TBPe*** is given by the ratio of $\frac{\Delta OD}{\Delta OD_{Ref}}$ at a selected wavelength (Fig. 3D). Considering the widely accepted $\Phi_{ISC,Ref}$ value for $[Os(phen)_3](PF_6)_2$ as 1, a Φ_{ISC} of 0.16 for **BDP-Br** was estimated (see eqn (1) and the ESI† for more experimental details). Based on the literature data that unsubstituted BODIPY shows negligible ISC,[47] herein it clearly appears that ISC is substantially accelerated for **BDP-Br**, allowing us to employ this BODIPY derivative as the sensitizer for triplet energy transfer-driven chemistry. The overall higher fluorescence quantum yield and a longer singlet lifetime of **BDP** compared to those of **BDP-Br** allow us to attribute the increased ISC quantum yield mainly to the heavy atom effect of the bromine atom rather than the fluorophenyl sulfide moiety (see Table 1 and Table S1, ESI†). The favorable absorption properties of **BDP-Br** with only one dominant absorption band in the green region and weak absorptivity in the blue region (*vide supra*) together with its high photostability make it a suitable candidate for a green-to-blue upconversion system.

BDP-Br and TBPe pair for TTA-UC

Considering the triplet state energy of **BDP-Br** as 1.68 eV, **TBPe** was selected as the suitable annihilator owing to its rather low triplet state energy of 1.53 eV[15] and high singlet-excited state energy of 2.81 eV, while the *tert*-butyl groups suppress unwanted excimer formation.[46] Given that ultrafast photoprocesses cannot be expected for our bimolecular UC system in the diluted solution,[48–50] we believed that laser flash photolysis (LFP) experiments in the ns–μs timescale range was the appropriate choice to further investigate the TTA-UC system (Fig. 4). Thus, a pronounced ground state bleach and a broad absorption band centered at around 640 nm and 450 nm were observed right after the laser pulse (λ_{exc} = 532 nm and ~10 ns pulse duration) (Fig. 4A). All signals decay to baseline with a natural lifetime of ~100 μs (Fig. 4B) and we assigned them to the triplet-excited **BDP-Br**. Stern–Volmer experiments were performed using **TBPe** as the quencher, yielding a TTEnT rate constant of 4.1×10^9 M^{-1} s^{-1} in line with the reported triplet energies (Fig. 4B). With the addition of **TBPe**, new absorption bands are detected in the TA spectrum (red) after **BDP-Br** has been fully quenched and the kinetic traces in Fig. 4A (inset) clearly demonstrate that quenching and photoproduct formation occur with identical rates. The new transient species shows absorption peaks at 484 nm and 453 nm which can be safely ascribed to the triplet state of **TBPe** (Fig. 4A, red spectrum).[46]

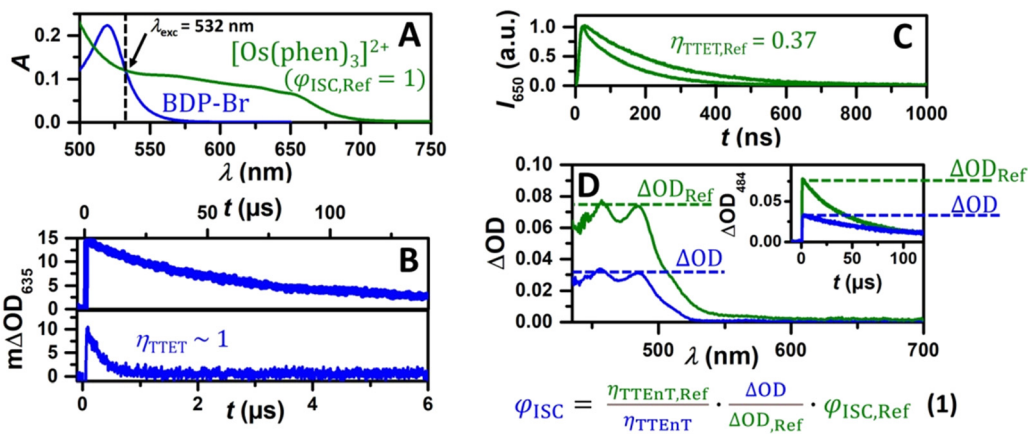

Fig. 3 Data sets used for the ISC quantum yield determination of **BDP-Br**. (A): Absorption spectra of deaerated 7 μM **BDP-Br** and deaerated 76 μM $[Os(phen)_3](PF_6)_2$ in ACN. (B): Kinetic traces of ^{3}**BDP-Br** in the absence (upper panel) and presence (lower panel) of 10 mM **TBPe**. (C): Kinetic measurements of the $[Os(phen)_3](PF_6)_2$ phosphorescence in the absence and presence of **TBPe**. (D): Transient absorption spectra of **BDP-Br** and $[Os(phen)_3](PF_6)_2$ with 10 mM **TBPe** recorded 1 μs after excitation with 532 nm laser pulses. Laser pulses of constant energy (12 mJ) were used in this series of experiments. Inset: kinetic measurements at 484 nm.

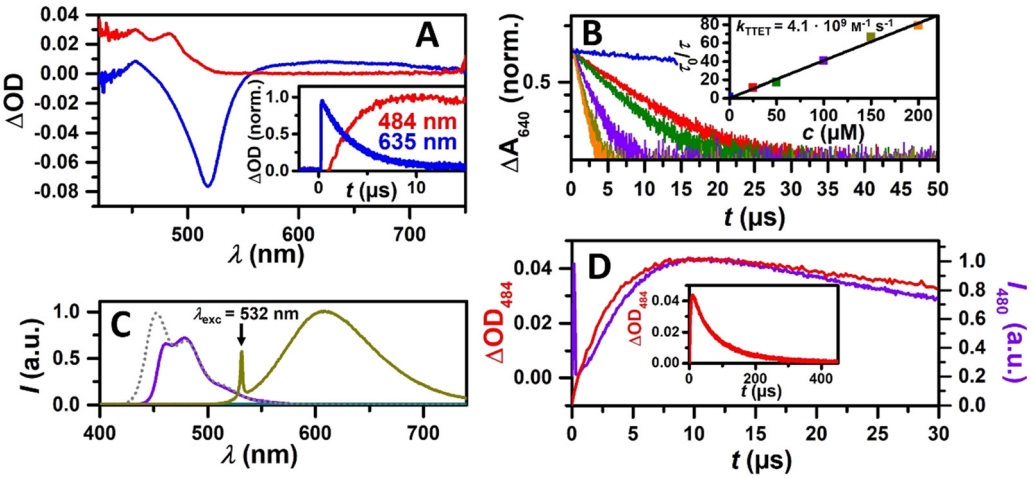

Fig. 4 Mechanistic LFP experiments using 532 nm laser pulses. If not stated otherwise, a solution of 9 μM **BDP-Br** and 100 μM **TBPe** in deaerated ACN was used. (A) TA spectra of **BDP-Br** in the presence (red) and absence (blue) of **TBPe** recorded after 2 μs (blue) or 30 μs (red). Inset: corresponding kinetic traces. (B) **BDP-Br** triplet quenching experiments with increasing **TBPe** concentrations. Inset: the corresponding Stern–Volmer plot. (C) Time-gated emission spectra of **TBPe** (green, integration time: 2–200 μs), **BDP-Br** (dark yellow, integration time: 0–100 ns) and **BDP-Br** *with* **TBPe** (purple, integration time: 2–200 μs). For comparison, an emission spectrum of a strongly diluted (1 μM) **TBPe** solution (dotted grey line) after direct excitation using 355 nm laser pulses is shown. (D) Kinetic traces of ^{3}**TBPe** at 484 nm and UC emission at 480 nm. Inset: the kinetic trace of ^{3}**TBPe** on a longer timescale.

Having established the TTEnT step, we then turned to the annihilation process. Individually, the sensitizer only shows fluorescence peaking at ~610 nm while no emission is detected from the annihilator after pulsed 532 nm excitation (Fig. 4C). When combined, however, emission signals with a spectral upshift respective to the excitation wavelength with maxima at 480 nm and 461 nm are detected. The detection time window (2–200 μs after excitation) allowed us to exclude the prompt emission of **TBPe** and **BDP-Br** such that delayed fluorescence expected for TTA-UC can be selectively observed. A spectrum containing the prompt emission of **TBPe** in a highly diluted solution is shown in Fig. 4C for comparison. It should be noted that inner filter effects in the absorption–emission overlap region become apparent at concentrations >10 μM (Fig. S11, ESI†). Kinetic traces of both the ^{3}**TBPe** absorption at 484 nm and the ^{1}**TBPe*** emission concurrently reach a maximum at ~11 μs (Fig. 4D). The faster increase and decrease of the UC emission compared to the triplet concentration is in line with the bimolecular nature of the annihilation process and provides further evidence for TTA-UC.[51]

In addition to the time-resolved studies that provided deep insights into the novel TTA-UC system, we investigated the UC efficiency using a 514 nm cw laser for excitation (Fig. 5). The UC emission peaking at 484 nm gradually enhanced with increasing laser intensity (10–100 mW). A spectral upshift of 0.40 eV was observed when the singlet-excited state energy of **TBPe** and the excitation wavelength (almost perfectly corresponding to the **BDP-Br** absorption maximum) were considered. To determine the UC quantum yield, Φ_{UC}, $[(Ru(bpy)_3](PF_6)_2$ was used as the reference system (see the ESI† for details of the method).[52] As depicted in the inset of Fig. 5, the Φ_{UC} for our metal-free system (with a theoretical limit of 50%) was found to reach a maximum of 2.7%. Despite the fact that this value was lower

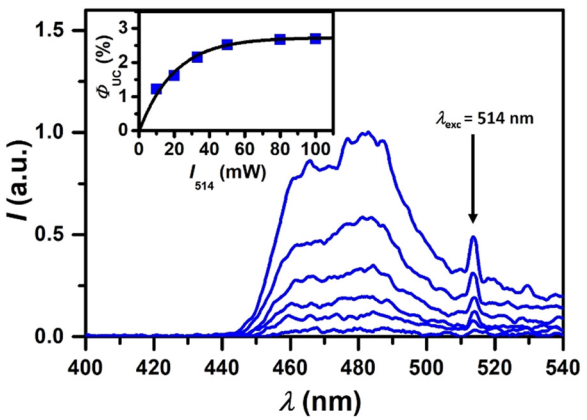

Fig. 5 Photon upconversion studies of 28 μM **BDP-Br** and 100 μM **TBPe** in deaerated ACN using a 514 nm cw laser for excitation. Main plot: UC Emission spectra with increasing laser intensity. Inset: the external UC quantum yield plotted against the laser intensity. See the text and ESI† for details.

than others from quantum-yield-optimized systems, the performance of the current TTA-UC system to act as the photocatalyst to drive challenging photoredox reactions appeared to be sufficient since well-known bimolecular systems that show Φ_{UC} well below 1% were able to trigger photochemical transformations such as reductive pollutant degradation.[53] Furthermore, the moderate quantum yield is likely compensated by the very high sensitizer and annihilator photostability (*vide supra*).

Application of the BDP-Br/TBPe system to photoredox catalysis

Several biphotonic excitation strategies in photoredox catalysis have been developed over the last few years in order to address critical bond activations or electron transfers under mild

conditions and using lower-energy visible light. Reactions such as two-photon absorption (TPA)[54] and consecutive photo-induced electron transfer (conPET)[55] can be carried out using a single photocatalyst. In the case of TTA-UC, a bimolecular system governs the catalytic cycle by the energy input of two photons where the primary photosensitizer transfers the absorbed energy to the co-catalyst (annihilator). Although the application of this technology to chemical transformations has been recently reviewed,[13] there is still plenty of room concerning the employment of improved systems. Therefore, in view of the outstanding TTA-UC properties of the **BDP-Br/TBPe** system, this couple was embedded as the photocatalyst into different challenging intermolecular coupling reactions.

To this end, we first explored the feasibility of activating 2-acetyl-5-chlorothiophene as the model reagent with visible light employing the **BDP-Br/TBPe** system. Quenching experiments were carried out by means of transient absorption spectroscopy (TAS) under conditions that are similar to those of the photocatalytic studies (Fig. 6A). Clearly, the delayed fluorescence intensity of **TBPe** gradually decreased in the presence of increasing amounts of the quencher. Indeed, the Stern–Volmer analysis of delayed emission quenching (Fig. 6A inset) revealed a K_{SV} of 117 M^{-1}; taking into account this value and the **TBPe** singlet lifetime (τ_F = 5 ns in ACN/DMA 4/1 v/v, see the ESI† for details), the fluorescence quenching rate constant, $k_q(S_1)$, was found to be 2.3 × 10^{10} M^{-1} s^{-1}, indicating that the target compound quenches the delayed ^{1}**TBPe*** with a diffusion-controlled rate. A very similar Stern–Volmer constant (K_{SV} = 135 M^{-1}) was obtained for ^{1}**TBPe*** quenching by 2-acetyl-5-chlorothiophene upon the direct excitation of **TBPe** (λ_{exc} = 405 nm) in neat ACN, supporting the UC-driven activation mechanism.

To further demonstrate the interaction between TTA-generated ^{1}**TBPe*** and 2-acetyl-5-chlorothiophene through an initial electron transfer step and to identify possible transient intermediates, additional time-resolved studies were performed (Fig. 6B). Hence, irradiation of the **BDP-Br/TBPe** system (λ_{exc} = 532 nm) in the presence of 2-acetyl-5-chlorothiophene was carried out. Interestingly, a new absorption band at *ca.* 560 nm was clearly observed which was safely ascribed to the **TBPe** radical cation (**TBPe**$^{\bullet+}$) based on the literature data.[56] From the temporal profile at 560 nm (Fig. 6C), a lifetime on the order of 400 μs was estimated for this intermediate.

In addition, thermodynamic analysis for ET processes strongly supported these data. The free energy change (ΔG_{ET} in kcal mol^{-1}) associated with the ET process was estimated by the application of the Weller equation.[57] The oxidation potential (E°(**TBPe**$^{\bullet+}$/**TBPe**)) of **TBPe** (Fig. 6D) and its singlet and triplet energy ($E^*(S_1$ or $T_1)$, for details see the ESI†) were experimentally obtained. Their corresponding values are 0.88 V *vs.* SCE, 64.6 and 34.6 kcal mol^{-1}, respectively. The resulting excited-state oxidation potential for the **TBPe**'s S_1 state is as high as −1.93 V *vs.* SCE, which should permit challenging photocatalytic reductions *via* TTA-UC.

Considering the reduction potential of the model reagent 2-acetyl-5-chlorothiophene (−1.66 V *vs.* SCE),[58] the ΔG_{ET} (S_1) and ΔG_{ET} (T_1) values were estimated as −6.0 kcal mol^{-1} and +23.9 kcal mol^{-1}, respectively. Therefore, the activation of 2-acetyl-5-chlorothiophene by delayed ^{1}**TBPe*** would be an exergonic process, whereas the mechanism from ^{3}**TBPe*** is

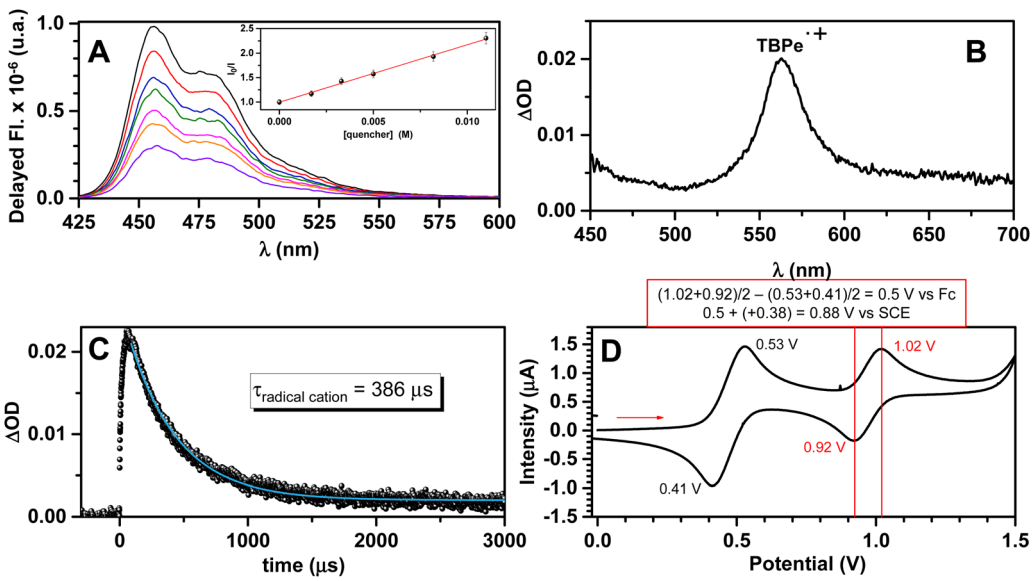

Fig. 6 Activation of the model reagent by delayed fluorescence ^{1}**TBPe***. (A): Delayed fluorescence spectra of a mixture of **BDP-Br** (0.1 mM) and **TBPe** (1 mM) in anaerobic ACN/DMA (4/1 v/v) solution recorded 2 μs after the laser pulse (λ_{exc} = 532 nm) in the presence of increasing amounts of 2-acetyl-5-chlorothiophene (up to 11 mM); inset: the Stern–Volmer plot to obtain k_q (S_1); experimental errors were lower than 5% of the obtained values. (B): TAS measurements (λ_{exc} = 532 nm) of **BDP-Br** (0.1 mM) and **TBPe** (1 mM) in the anaerobic ACN solution in the presence of 10 mM of 2-acetyl-5-chlorothiophene recorded 140 μs after the laser pulse. (C): Temporal profile of the **TBPe** radical cation monitored at 560 nm. The blue line is the fit function used to estimate the lifetime. (D): Cyclic voltammogram for an ACN solution of **TBPe** (0.1 mM).

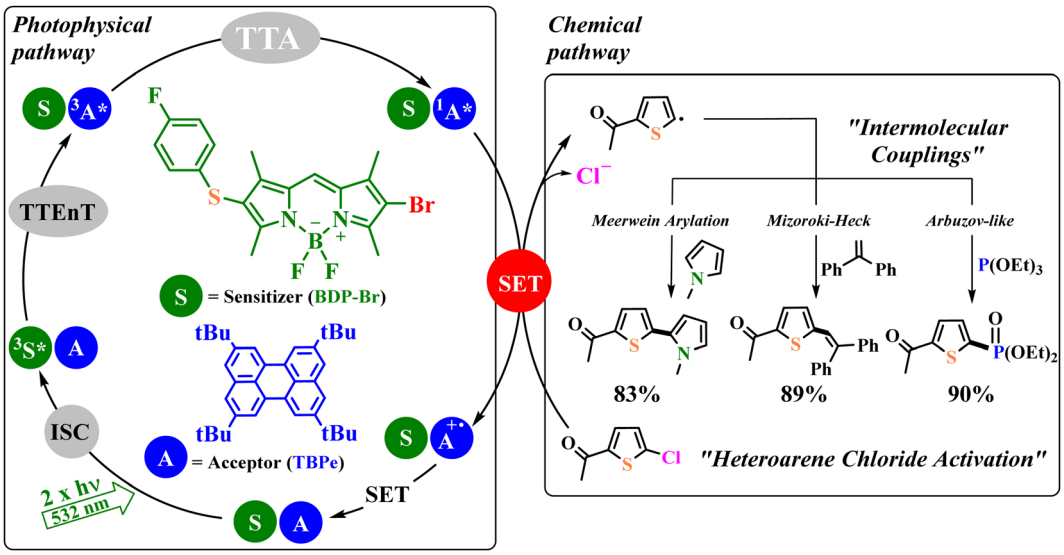

Fig. 7 Mechanism of TTA-UC enabled by the **BDP-Br**(S)/**TBPe**(A) pair and its adaptation to photoredox catalysis through a SET-initiated reductive activation of an aryl chloride. Involvement of sequential processes ISC, TTEnT, TTA and SET as key steps. ISC = intersystem crossing; TTEnT = triplet–triplet energy transfer; TTA = triplet–triplet annihilation; SET = single-electron transfer.

thermodynamically unfeasible. Same calculations were indeed performed for **BDP-Br** with the question whether this species could act as an activator. Considering the experimental data of **BDP-Br** (E_{ox} = + 1.23 V *vs.* SCE, $E(S_1)$ = 52.1 kcal mol^{-1} and $E(T_1)$ = 38.7 kcal mol^{-1}, see the ESI† for details), both ΔG_{ET} (S_1) and ΔG_{ET} (T_1) were estimated as positive values (+13.8 kcal mol^{-1} and +27.2 kcal mol^{-1}, respectively), ruling out any ET from the excited **BDP-Br**.

These results allowed us to conclude that the activation of 2-acetyl-5-chlorothiophene was successfully powered using the TTA-UC system through a SET process (Fig. 7). Thus, the conversion of low energy light (2.3 eV) into the higher energy delayed ^{1}**TBPe*** (2.8 eV) allowed the one-electron injection, giving rise to the formation of the unstable radical anion of the model compound which rapidly released chloride to afford the corresponding heteroarene radical. This reactive species could be now trapped by adequate nucleophiles to produce complex compounds (Fig. 7). Therefore, we investigated the application of this cascade of processes (TTA-UC + SET + intermolecular coupling) to different important reactions such as the Meerwein arylation or the Mizoroki–Heck reaction in order to functionalize the thiophene ring by C–C coupling and the Arbuzov-like reaction to construct the corresponding thiophene phosphonate.

The photocatalyzed Meerwein arylation is a classic reaction in which aryl diazonium salts were employed as aryl radical precursors.[59] However, most of these species are not neither commercially available nor stable in the presence of air, being their employment sometimes detrimental. In this context, aryl halides were used as alternative electrophilic reagents in such reactions. Recently, a TTA-UC system based on the diiodo-BOPHY-like derivative as the sensitizer and 9,10-diphenylanthracene as the annihilator photocatalyzed the coupling reaction between our model compound (2-acetyl-5-chlorothiophene) and *N*-methylpyrrole, yielding 62% of the final biaryl product.[60] The instability of the sensitizer under the irradiation conditions (λ_{exc} = 450 nm) could be an important factor for the incomplete conversion of the starting material or the lack of more product formation. Thus, we focused our attention on the same reaction utilizing **BDP-Br**/**TBPe** as the TTA-UC photocatalytic system. Optimal conditions (see Table S2 for the optimization of the model reaction in the ESI†) involved catalytic amounts of **BDP-Br** (2% mol) and **TBPe** (10% mol), with pulsed laser irradiation in the green region at 532 nm in ACN/DMA (4/1 v/v) solution for 4 hours under anaerobic conditions. The result was markedly improved to that previously obtained with an 83% yield of the final product. It is worth mentioning that the ACN/DMA mixture as a solvent was found to be ideal not only for enhancing the selectivity of the process but also for favoring the complete dissolution of **TBPe**.

At the same shape, TTA-UC technology was very recently applied to the photocatalyzed Mizoroki–Heck reaction to obtain substituted triarylethylenes using aryl halides (especially bromides) as aryl radical precursors.[61] With the optimizing conditions stated above, our model compound was subjected to green-light photolysis (λ_{exc} = 532 nm) in the presence of diphenylethylene as the trapping agent and catalytic amounts of the **BDP-Br**/**TBPe** system (for detailed information on the reaction conditions, see the ESI†). Full conversion of the starting material was observed after 4 hours of irradiation and an excellent 89% yield of the final product was obtained. This finding notably improved the previous example (*i.e.*, 49%)[61] despite the lower-energy light input and the shortened irradiation time, confirming the efficiency of the photocatalytic activity of the TTA-UC couple.

Biphotonic-based methods for the C–P bond formation of (hetero)aryl halides with trialkyl phosphite *via* the visible-light-induced photo-Arbuzov reaction have been barely explored.[58,62]

In particular, these studies followed a consecutive photoinduced electron transfer (ConPET) mechanism using organic dyes as photocatalysts together with a sacrificial agent as the base. As far as we are aware, the photo-Arbuzov reaction catalyzed using a TTA-UC system has not been attempted yet and we were interested whether this protocol could be a powerful strategy to forge new C(sp^2)–P bonds under mild conditions. The phosphorylation of the model compound, 2-acetyl-5-chlorothiophene, was thus carried out in the presence of **BDP-Br/TBPe** as the TTA-UC photocatalytic system under the optimal conditions (for detailed information on the reaction conditions, see the ESI†). Interestingly, the targeted product was obtained with an excellent 90% yield, which was comparable to the previously reported value (91%)[58] in spite of the absence of sacrificial agents.

Conclusions

In summary, we have developed a purely organic upconversion system that efficiently catalyzes challenging reductions under green-light excitation conditions. Our tailor-made BODIPY sensitizer shows efficient triplet formation and energy transfer to the selected annihilator, while possessing outstanding photostability properties compared to the most famous photoactive metal complex as the reference. The excited annihilator singlet obtained *via* upconversion is a strong photoreductant providing about 2 V of reductive power. Given the low price and durability of green light sources such as frequency-doubled Nd:YAG lasers (which are also the key components of most commercial laser pointers) and green diode-based lamps compared to blue lasers and diodes, our approach should be within reach for most photochemical laboratories to activate substrates in a selective fashion under metal-free conditions.

Author contributions

All authors discussed the results and reviewed the manuscript.

Conflicts of interest

There are no conflicts of interest.

Acknowledgements

We thank the Generalitat Valenciana (project CIDEGENT/2018/044), the Spanish Government (project PID2019-105391GB-C22 funded by MCIN/AEI/10.13039/501100011033), the German Federal Environmental Foundation (DBU, PhD fellowship to T. J. B. Z., grant number 20022/028) and the German Research Foundation (DFG, grant number KE 2313/3-1) for financial support. We also thank Prof. Julia Pérez-Prieto for spectroscopic facilities.

References

1 A. L. Hagstrom, H.-L. Lee, M.-S. Lee, H.-S. Choe, J. Jung, B.-G. Park, W.-S. Han, J.-S. Ko, J.-H. Kim and J. H. Kim, *ACS Appl. Mater. Interfaces*, 2018, **10**, 8985–8992.
2 M. Barawi, F. Fresno, R. Pérez-Ruiz and V. A. de la Peña O'Shea, *ACS Appl. Energy Mater.*, 2019, **2**, 207–211.
3 V. Gray, D. Dzebo, M. Abrahamsson, B. Albinsson and K. Moth-Poulsen, *Phys. Chem. Chem. Phys.*, 2014, **16**, 10345–10352.
4 T. F. Schulze and T. W. Schmidt, *Energy Environ. Sci.*, 2015, **8**, 103–125.
5 L. Frazer, J. K. Gallaher and T. W. Schmidt, *ACS Energy Lett.*, 2017, **2**, 1346–1354.
6 T. Dilbeck and K. Hanson, *J. Phys. Chem. Lett.*, 2018, **9**, 5810–5821.
7 Y. Zhou, C. Ruchlin, A. J. Robb and K. Hanson, *ACS Energy Lett.*, 2019, **4**, 1458–1463.
8 H.-L. Lee, J. H. Park, H.-S. Choe, M.-S. Lee, J.-M. Park, N. Harada, Y. Sasaki, N. Yanai, N. Kimizuka, J. Zhu, S. H. Bhang and J.-H. Kim, *ACS Appl. Mater. Interfaces*, 2019, **11**, 26571–26580.
9 Q. Liu, M. Xu, T. Yang, B. Tian, X. Zhang and F. Li, *ACS Appl. Mater. Interfaces*, 2018, **10**, 9883–9888.
10 S. H. C. Askes, M. S. Meijer, T. Bouwens, I. Landman and S. Bonnet, *Molecules*, 2016, **21**, 1460.
11 Q. Liu, T. Yang, W. Feng and F. Li, *J. Am. Chem. Soc.*, 2012, **134**, 5390–5397.
12 C. Wohnhaas, A. Turshatov, V. Mailänder, S. Lorenz, S. Baluschev, T. Miteva and K. Landfester, *Macromol. Biosci.*, 2011, **11**, 772–778.
13 R. Pérez-Ruiz, *Top. Curr. Chem.*, 2022, **380**(23), 1–12.
14 F. Glaser, C. Kerzig and O. S. Wenger, *Angew. Chem., Int. Ed.*, 2020, **59**, 10266–10284.
15 B. D. Ravetz, A. B. Pun, E. M. Churchill, D. N. Congreve, T. Rovis and L. M. Campos, *Nature*, 2019, **565**, 343–346.
16 S. Wen, J. Zhou, P. J. Schuck, Y. D. Suh, T. W. Schmidt and D. Jin, *Nat. Photonics*, 2019, **13**, 828–838.
17 M. Wu, T.-A. Lin, J. O. Tiepelt, V. Bulović and M. A. Baldo, *Nano Lett.*, 2021, **21**, 1011–1016.
18 E. Radiunas, S. Raišys, S. Juršėnas, A. Jozeliūnaitė, T. Javorskis, U. Šinkevičiūtė, E. Orentas and K. Kazlauskas, *J. Mater. Chem. C*, 2020, **8**, 5525–5534.
19 J. Zhou, Q. Liu, W. Feng, Y. Sun and F. Li, *Chem. Rev.*, 2015, **115**, 395–465.
20 J. Zhao, W. Wu, J. Sun and S. Guo, *Chem. Soc. Rev.*, 2013, **42**, 5323–5351.
21 Y. Y. Cheng, T. Khoury, R. G. C. R. Clady, M. J. Y. Tayebjee, N. J. Ekins-Daukes, M. J. Crossley and T. W. Schmidt, *Phys. Chem. Chem. Phys.*, 2010, **12**, 66–71.
22 S. Hoseinkhani, R. Tubino, F. Meinardi and A. Monguzzi, *Phys. Chem. Chem. Phys.*, 2015, **17**, 4020–4024.
23 D. Dzebo, K. Moth-Poulsen and B. Albinsson, *Photochem. Photobiol. Sci.*, 2017, **16**, 1327–1334.
24 R. Weiss, Z. A. VanOrman, C. M. Sullivan and L. Nienhaus, *ACS Mater. Au*, 2022, **2**, 641–654.

25 Z. A. VanOrman, C. R. Conti, G. F. Strouse and L. Nienhaus, *Chem. Mater.*, 2021, **33**, 452–458.
26 Z. A. VanOrman, H. K. Drozdick, S. Wieghold and L. Nienhaus, *J. Mater. Chem. C*, 2021, **9**, 2685–2694.
27 N. Kiseleva, P. Nazari, C. Dee, D. Busko, B. S. Richards, M. Seitz, I. A. Howard and A. Turshatov, *J. Phys. Chem. Lett.*, 2020, **11**, 2477–2481.
28 M. Yang, S. Sheykhi, Y. Zhang, C. Milsmann and F. N. Castellano, *Chem. Sci.*, 2021, **12**, 9069–9077.
29 C. Wang, F. Reichenauer, W. R. Kitzmann, C. Kerzig, K. Heinze and U. Resch-Genger, *Angew. Chem., Int. Ed.*, 2022, **61**, e202202238(3 of 8).
30 W. Chen, F. Song, S. Tang, G. Hong, Y. Wu and X. Peng, *Chem. Commun.*, 2019, **55**, 4375–4378.
31 Y. Hou, J. Liu, N. Zhang and J. Zhao, *J. Phys. Chem. A*, 2020, **124**, 9360–9374.
32 P. Yuster and S. I. Weissman, *J. Chem. Phys.*, 1949, **17**, 1182.
33 T. Yogo, Y. Urano, Y. Ishitsuka, F. Maniwa and T. Nagano, *J. Am. Chem. Soc.*, 2005, **127**, 12162–12163.
34 X. Xiao, W. Tian, M. Imran, H. Cao and J. Zhao, *Chem. Soc. Rev.*, 2021, **50**, 9686–9714.
35 J. M. Lee, J.-M. Park, J. Ho Yoon, J.-H. Kim and J. P. Kim, *ChemPhotoChem*, 2023, e202200326.
36 K. Chen, Y. Dong, X. Zhao, M. Imran, G. Tang, J. Zhao and Q. Liu, *Front. Chem.*, 2019, **7**, 821.
37 N. A. Bumagina, E. V. Antina, A. A. Ksenofontov, L. A. Antina, A. A. Kalyagin and M. B. Berezin, *Coord. Chem. Rev.*, 2022, **469**, 214684.
38 D. Alves, R. G. Lara, M. E. Contreira, C. S. Radatz, L. F. B. Duarte and G. Perin, *Tetrahedron Lett.*, 2012, **53**(26), 3364–3368.
39 E. V. Antina, M. B. Berezin, N. A. Dudina, S. L. Burkova and A. Y. Nikonovab, *Russ. J. Inorg. Chem.*, 2014, **59**(10), 1427–1434.
40 E. Palao, T. Slanina and P. Klán, *Chem. Commun.*, 2016, **52**, 11951–11954.
41 K. N. Solov'ev and E. A. Borisevich, *Phys.-Usp.*, 2005, **48**, 231–253.
42 X.-F. Zhang, X. Yang, K. Niu and H. Geng, *J. Photochem. Photobiol., A*, 2014, **285**, 16–20.
43 J. B. Bilger, C. Kerzig, C. B. Larsen and O. S. Wenger, *J. Am. Chem. Soc.*, 2021, **143**, 1651–1663.
44 M.-S. Bertrams and C. Kerzig, *Chem. Commun.*, 2021, **57**, 6752–6755.
45 P. Müller and K. Brettel, *Photochem. Photobiol. Sci.*, 2012, **11**, 632–636.
46 C. Ye, V. Gray, K. Kushwaha, S. K. Singh, P. Erhart and K. Börjesson, *Phys. Chem. Chem. Phys.*, 2020, **22**, 1715–1720.
47 A. Schmitt, B. Hinkeldey, M. Wild and G. Jung, *J. Fluoresc.*, 2009, **19**, 755–758.
48 C. Wang, M. Sun, H. Wang and G. Zhao, *J. Phys. Chem. Lett.*, 2023, **14**, 164–169.
49 C. Wang, L. Ma, S. Wang and G. Zhao, *J. Phys. Chem. Lett.*, 2021, **12**, 12129–12134.
50 C. Wang, Y. Liu, X. Feng, C. Zhou, Y. Liu, X. Yu and G. Zhao, *Angew. Chem., Int. Ed.*, 2019, **59**, 11642–11646.
51 Y. Murakami and K. Kamada, *Phys. Chem. Chem. Phys.*, 2021, **23**, 18268–18282.
52 K. Suzuki, A. Kobayashi, S. Kaneko, K. Takehira, T. Yoshihara, H. Ishida, Y. Shiina, S. Oishic and S. Tobita, *Phys. Chem. Chem. Phys.*, 2009, **11**, 9850–9860.
53 B. Pfund, D. M. Steffen, M. R. Schreier, M.-S. Bertrams, C. Ye, K. Börjesson, O. S. Wenger and C. Kerzig, *J. Am. Chem. Soc.*, 2020, **142**, 10468–10476.
54 C. Kerzig, X. Guo and O. S. Wenger, *J. Am. Chem. Soc.*, 2019, **141**, 2122–2127.
55 I. Ghosh, T. Ghosh, J. I. Bardagi and B. König, *Science*, 2014, **346**, 725–728.
56 C. A. Steren, H. van Willigen, L. BiczoÂk, N. Gupta and H. Linschitz, *J. Phys. Chem.*, 1996, **100**, 8920–8926.
57 ΔG_{ET} (kcal mol^{-1}) = 23.06 x (E_{ox} – E_{RED}) – $E^*(S_1$ or $T_1)$: A. Weller, *Z. Phys. Chem.*, 1982, **133**, 93–98.
58 J. C. Herrera-Luna, D. Díaz Díaz, M. C. Jiménez and R. Pérez-Ruiz, *ACS Appl. Mater. Interfaces*, 2021, **13**, 48784–48794.
59 D. Prasad Hari and B. König, *Angew. Chem., Int. Ed.*, 2013, **52**, 4734–4743.
60 C. G. López-Calixto, M. Liras, V. A. de la Peña O'Shea and R. Pérez-Ruiz, *Appl. Catal., B*, 2018, **237**, 18–23.
61 F. Garnes-Portolés, R. Greco, J. Oliver-Meseguer, J. Castellanos-Soriano, M. C. Jiménez, M. López- Haro, J. C. Hernández-Garrido, M. Boronat, R. Pérez-Ruiz and A. Leyva-Pérez, *Nat. Catal.*, 2021, **4**, 293–303.
62 R. S. Shaikh, S. J. S. Düsel and B. König, *ACS Catal.*, 2016, **6**, 8410–8414.